

Physiological Research Pre-Press Article

1 **Title:** Three types of ion channels in the cell membrane of mouse fibroblasts

2 **Authors:** Mateusz Koselski¹, Anna Olszewska², Anna Hordyjewska³, Teresa Małecka-
3 Massalska², Kazimierz Trebacz¹

4 **Affiliations of authors:**

5 ¹Department of Biophysics, Institute of Biology and Biochemistry, Maria Curie-
6 Skłodowska University, Lublin, Poland

7 ²Department of Human Physiology, Medical University of Lublin, Lublin, Poland

8 ³Department of Medical Chemistry, Medical University of Lublin, Lublin, Poland

9 **Corresponding author:**

10 Mateusz Koselski, Department of Biophysics, Institute of Biology and Biochemistry,
11 Maria Curie-Skłodowska University, Akademicka 19, 20-033 Lublin, Poland, e-mail:
12 mateusz.koselski@poczta.umcs.lublin.pl

13 **Short title:** Ion channels of mouse fibroblasts

14

15

16

17

18

19

20

21 **Summary**

22 Patch clamp recordings carried out in the inside-out configuration revealed
23 activity of three kinds of channels: nonselective cation channels, small-conductance K⁺
24 channels, and large-conductance anion channels. The nonselective cation channels did
25 not distinguish between Na⁺ and K⁺. The unitary conductance of these channels reached
26 28 pS in a symmetrical concentration of 200 mM NaCl. A lower value of this parameter
27 was recorded for the small-conductance K⁺ channels and in a 50-fold gradient of K⁺
28 (200 mM/4 mM) it reached 8 pS. The high selectivity of these channels to potassium
29 was confirmed by the reversal potential (-97 mV), whose value was close to the
30 equilibrium potential for potassium (-100 mV). One of the features of the large-
31 conductance anion channels was high conductance amounting to 493 pS in a
32 symmetrical concentration of 200 mM NaCl. The channels exhibited three
33 subconductance levels. Moreover, an increase in the open probability of the channels at
34 voltages close to zero was observed. The anion selectivity of the channels was low,
35 because the channels were permeable to both Cl⁻ and gluconate - a large anion.
36 Research on the calcium dependence revealed that internal calcium activates
37 nonselective cation channels and small-conductance K⁺ channels, but not large-
38 conductance anion channels.

39 **Keywords:** patch-clamp, mouse fibroblast, cell membrane, cation channels, K⁺
40 channels, anion channels

41

42

43

44 **Introduction**

45 Fibroblasts are the most common type of cells found in connective tissue. They
46 are defined as cells that synthesize and secrete collagen proteins and they are also
47 believed to be an essential source of many other extracellular matrix components
48 (Theerakittayakorn and Bunprasert 2011). Animal or human fibroblasts grow well in
49 cultures and are readily available for experiments; therefore, they have been widely
50 used for investigation of many physiological and biochemical responses. Learning more
51 about their general physiology and ion channel activity in particular is very important
52 (Estacion 1991).

53 Different types of cation- and anion-selective channels were characterized in
54 mouse fibroblasts using patch-clamp techniques. Voltage-dependent calcium currents
55 were detected in mouse Swiss 3T3 fibroblasts (Peres *et al.* 1988a, Peres *et al.* 1988b).
56 These rapidly activating and fully inactivating inward currents were evoked by
57 depolarization from negative voltages and were similar to low-voltage T-type calcium
58 channels activated by small depolarization of the cell membrane potential (Perez-Reyes
59 2003). Weak permeability of recorded channels to other than calcium divalent cations
60 was confirmed by reduction of the currents by Cd²⁺ (Peres *et al.* 1988a), and slight
61 reduction of the currents recorded after replacement of external Ca²⁺ with Ba²⁺ (Peres *et*
62 *al.* 1988b). On the other hand, after elimination of all divalent cations from the external
63 solution, permeability to monovalent cations was observed. A lack of sensitivity to
64 calcium channel blockers like nitrendipine and verapamil was also characteristic for the
65 channels. In the study of Peres and coworkers, an absence of calcium-activated K⁺
66 channels was reported (Peres *et al.* 1988a), but such channels were recorded in the
67 mouse fibroblastic line LMTK-, a thymine-kinase-deficient strain of L cells (Hosoi and

68 Slaymann 1985). In turn, cell-attached and inside-out patch recording carried out by
69 Frace and Gargus indicated that the predominant channel of LMTK- was a nonselective
70 calcium- and voltage independent cation channel, permeable equally to Na^+ , K^+ , and
71 Cs^+ and non-permeable to anions or divalent cations (Frace and Gargus 1989). Apart
72 from mouse LMTK- cells, Ca^{2+} dependent K^+ currents were recorded also in NIH3T3
73 mouse fibroblasts (Repp *et al.* 1998). The channels were activated by lysophosphatidic
74 acid and showed voltage-independence and sensitivity to the K^+ channels blockers
75 (charybdotoxin, margatoxin, and iberiotoxin). The whole cell patch-clamp recordings
76 carried out in mouse LMTK-fibroblasts indicated existence of volume-sensitive Cl^-
77 currents whose activation is delayed by high intracellular chloride (Doroshenko 1999).
78 Moreover, Cl^- conductance of these channels is affected by protein tyrosine phosphatase
79 inhibitors (Thoroed *et al.* 1999). Mouse skin fibroblasts 3T3-L1 were also used for
80 patch-clamp investigations by Goodwin and coworkers. However, as reported, there
81 were difficulties in obtaining results, since poor seals in both cell-attached and excised
82 inside-out configurations and a low success rate in finding channels (<10%) were
83 observed. The channels, rarely recorded in the cell-attached configuration, were not
84 voltage-dependent and probably K^+ impermeable (Goodwin *et al.* 1998).

85 Ion channels play an important physiological role. Many functions and possible
86 roles of some channels are discussed. A big number of ion channelopathies, especially
87 potassium, calcium, and sodium channel diseases, affect the neuromuscular system and
88 cause diseases such as epilepsy, myotonia, or cardiac arrhythmias (Fiske *et al.* 2006).
89 Defects in ion channels may cause either a gain or a loss of channel function. Changes
90 in the ion channel composition have been observed in fibroblasts from patients with
91 Alzheimer's disease (AD). Etcheberrigaray and coworkers indicated an absence of a

92 113-pS tetraethylammonium (TEA)-sensitive K⁺ channel in AD fibroblasts, while they
93 were present in control cells (Etcheberrigaray *et al.* 1993).

94 This paper describes ion channels found in the mouse L 929 fibroblastic cell
95 line, which is widely used in many experimental aspects. Patch-clamp recordings
96 carried out in the inside-out configuration allowed characterization of three different
97 types of channels, which are important for transport of monovalent cations and anions
98 through the cell membrane.

99 **Materials and methods**

100 **Cell culture and culture media**

101 The experiment was conducted on a reference cell line L929 (cell line origin -
102 mouse C3H/An connective tissue). The L929 cell line was obtained from ATCC
103 (specification - NCTC clone 929 [L cell, L-929, derivative of Strain L] (ATCC® CCL-
104 1™), http://www.lgcstandards-atcc.org/products/all/CCL-1.aspx?geo_country=pl). Cell
105 cultures were grown at 37°C in a humidified atmosphere comprising 5% CO₂ in the air.
106 L929 cultures were maintained at density of 2-4 x 10⁴ cell/ml in exponential growth
107 serum free conditions containing Modified Eagle Medium (MEM, Pan-Biotech, P04-
108 08500; [http://www.pan-biotech.de/en/media-en/cell-culture-media/mem-](http://www.pan-biotech.de/en/media-en/cell-culture-media/mem-overview/mem-with-earle-s-salts)
109 supplemented with 5% fetal bovine serum (Pan-
110 Biotech, P30-1985, <http://www.pan-biotech.de/en/sera/treated-sera>), 100 U/ml of
111 penicillin, 100 µg/ml of streptomycin, 0.25 µg/ml of amphotericin B (Pan-Biotech, P06-
112 07300; <http://www.pan-biotech.de/en/reagents/antibiotics-and-antifungal-drugs>), and
113 routinely passaged every second day using 0.25% trypsin (Pan-Biotech, P10-027500;
114 <http://www.pan-biotech.de/en/reagents/enzymes-for-cell-dissociation/trypsin-and-others>). Cell viability was assessed by the ability to exclude trypan blue dye (Sigma-

116 Aldrich, Germany, T6146). Cells for patch-clamp experiments were transferred to
117 plastic 60-mm tissue culture dishes and grown in the same conditions for up 2 days.

118 **Solutions used in the patch-clamp recordings**

119 Patch-clamp recordings were made in the inside-out configuration in solutions
120 initially containing symmetrical (in the pipette and in the bath) concentrations of 200
121 mM NaCl, 4 mM KCl, 2 mM CaCl₂, 2 mM MgCl₂, pH 7.3 buffered with 10 mM
122 HEPES/NaOH (abbreviation of these solutions used in figure legends and text - 200 Na⁺
123 pipette /200 Na⁺ _{bath}). The selectivity of the channels was examined in an NaCl gradient
124 after tenfold reduction of NaCl in the bath by application of 20 mM NaCl, 4 mM KCl, 2
125 mM CaCl₂, 2 mM MgCl₂, pH 7.3 buffered with 10 mM HEPES/NaOH (abbreviation -
126 200 Na⁺ pipette /200 Na⁺ _{bath}). Permeability of cation-permeable channels to potassium was
127 studied by replacement of NaCl in the bath with KCl - of 200 mM KCl, 4 mM NaCl, 2
128 mM CaCl₂, 2 mM MgCl₂, pH 7.3 buffered with 10 mM HEPES/KOH (abbreviation -
129 200 Na⁺ pipette /200 K⁺ _{bath}). Permeability of anion-permeable channels to gluconate was
130 studied in 20 mM NaCl, 4 mM KCl, 2 mM CaCl₂, 2 mM MgCl₂, pH 7.3 buffered with
131 10 mM HEPES/NaOH in the bath and 200 mM Na-gluconate, 4 mM KCl, 2 mM CaCl₂,
132 2 mM MgCl₂, pH 7.3 buffered with 10 mM HEPES/NaOH in the pipette (abbreviation
133 - 200 Glu⁻ pipette / 32 Cl⁻ _{bath}). Calcium dependence of the channels was tested during
134 inside-out recordings by application of the solution containing 2 mM Ca²⁺ (200 mM
135 KCl, 4 mM KCl, 2 mM CaCl₂, 2 mM MgCl₂, pH 7.3 buffered with 10 mM
136 HEPES/KOH) by a micropipette placed close to the cytoplasmic side of the cell
137 membrane. Calcium was injected using a CellTram vario pump (Eppendorf). Before
138 calcium application, the recordings were carried out in 200 mM NaCl, 4 mM KCl, 2
139 mM CaCl₂, 2 mM MgCl₂, pH 7.3 buffered with 10 mM HEPES/NaOH in the pipette

140 and 200 mM KCl, 4 mM NaCl, 2 mM EGTA, 2 mM MgCl₂, pH 7.3 buffered with 10
141 mM HEPES/KOH in the bath (abbreviation - 200 Na⁺, 2 Ca²⁺ pipette/200 K⁺, 2 EGTA
142 bath). The osmolarity of solutions with a reduced ionic concentration was compensated
143 by adding sorbitol. Adjusting of the osmolarity was measured with a cryoscopic
144 osmometer (Osmomat 030, Gonotec).

145 **Patch-clamp measurements**

146 The patch pipettes and micropipettes used for injection of Ca²⁺ were prepared
147 from borosilicate glass capillary tubes with an outer diameter of 1.5 mm (Kwik-Fil,
148 TW150-4, World Precision Instruments), pulled by a universal puller (DMZ). The patch
149 pipette tip had an inside diameter of approx. 2 µm. An Ag-AgCl reference electrode
150 filled with 100 mM KCl was connected with the bath solution via a ceramic porous
151 bridge. The recordings were made by a patch-clamp amplifier EPC-10 (Heka
152 Elektronik) coupled with the Patchmaster software (Heka Elektronik). The signals were
153 recorded with a frequency of 10 kHz and filtered at 2 kHz. The recordings, which lasted
154 10 seconds or more (Fig. 5 and 6), were drawn by taking into account every tenth
155 measuring point. Elaboration of the current/voltage characteristics (I/V) and column
156 diagrams showing dependence of the open probability on the voltage applied was made
157 in SigmaPlot 9.0 (Systat Software Inc.). The slope of the I/V curve allowed calculation
158 of the unitary conductance of the channels. Open probability of the channels was
159 calculated in Fitmaster (Heka Elektronik).

160 **Statistical analysis**

161 Data presented in the I/V curves and P_o/V column charts are given as arithmetic
162 mean±standard error of the mean (SEM). The number of repeats (*n*) indicates the

163 number of patches tested. The open probability of a single channel was calculated as the
164 ratio of the open time and the total recording time (the sum of open and close time). In
165 the case of activity of more than one channel in the patch, the open probability was
166 divided by the number of active channels. Statistical significance was evaluated using a
167 *t*-test (for two groups) or ANOVA with Bonferroni post-hoc test (for more than two
168 groups). Data were compiled using SigmaStat (version 3.5). A value of *P* lower than
169 0.05 was considered statistically significant.

170 **Results**

171 **Nonselective cation channels**

172 The predominant type of ion currents recorded in the cell membrane of mouse
173 fibroblasts were those that passed through nonselective cation channels (Fig. 1A). The
174 activity of these channels was recorded in most (58%, 15 out of 26) of the patches tested
175 in the inside-out configuration in the symmetrical (in the bath and in the pipette)
176 concentration of 200 mM NaCl. In such conditions, the channels were active in negative
177 and positive voltages carrying the ions in both directions of the membrane. Their
178 unitary conductance (established from the slope of the I/V curve) reached 28 pS. The
179 value of this parameter was lower in the ten-fold gradient of NaCl (200 mM NaCl in the
180 pipette and 20 mM NaCl in the bath) and amounted to 25 pS (Fig. 1B). The conditions
181 used caused decline of the channel activity at positive voltages and an increase in the
182 open probability at negative voltages (Fig. 1D) and indicated that Na⁺ ions flowed
183 through the channels in accordance with their electrochemical gradient. The reversal
184 potential obtained from the I/V curve (Fig. 1C) shifted toward positive values and
185 reached 24 mV - a value closer to the equilibrium potential of sodium ($E_{Na} = 54$ mV)

186 than chloride ($E_{Cl} = -44$ mV) calculated on the basis of ion activities. The above results
187 indicated Na^+ over Cl^- selectivity of the channels.

188 The difference between the reversal potential obtained from the measurements
189 and E_{Na} , was the reason for a more detailed study of the low cation-selectivity of the
190 channels. In order to compare the selectivity of the channels to K^+ and Na^+ , a 50-fold
191 gradient facilitating outward K^+ currents and inward Na^+ currents was applied (Fig. 2A).
192 In such conditions, the reversal potential obtained from the I/V curve (Fig. 2C)
193 amounted to -1 mV, which proved that the channels did not distinguish K^+ and Na^+
194 ions. In comparison to the experiments carried out in symmetrical concentration 200
195 Na^+ , the exchange of 200 mM Na^+ on the cytoplasmic side to 200 mM K^+ caused an
196 increase in channel conductance from 28 pS (Fig. 1A, C) to 33 pS (Fig. 2A, C).

197 **Small-conductance K^+ channels**

198 Small-conductance K^+ channel activity was recorded in identical conditions as in
199 the earlier experiments carried out in the 50-fold gradient of K^+ and Na^+ (200 Na^+ pipette
200 /200 K^+ bath, Fig. 2B, D). These currents were recorded in 36% (5 of 14) of the patches.
201 The channel conductance was much lower than the conductance of nonselective cation
202 channels and amounted to 8 pS. The high selectivity of the channels to potassium was
203 confirmed by the value of the reversal potential obtained from the I/V curve (Fig. 2D),
204 which amounted to -97 mV - a value close to the equilibrium potential of potassium (-
205 100 mV).

206 **Large-conductance anion channels**

207 Apart from the channels described previously, large-conductance channels were
208 recorded. These channels recorded in the symmetrical concentration of 200 mM NaCl

209 (Fig. 3A, D) were active in 42% (11 of 26) of the patches. Interestingly, the channels
210 were not active immediately after excision, but required several minutes of polarization
211 of the patch (by 3-second impulses in the range from -80 mV to 80 mV with 20 mV
212 steps). A characteristic trait of the channels was their high conductance amounting to
213 493 pS. Tenfold reduction of the concentration of cytoplasmic NaCl caused reduction of
214 the conductance to 296 pS and also a shift of the reversal potential to -29 mV, indicating
215 Cl⁻ over Na⁺ selectivity of the channels (Fig. 3B, D). The channels were not highly
216 selective for chloride since their activity was not inhibited by the substitution of
217 cytoplasmic 200 mM Cl⁻ by 200 mM gluconate - an anion impermeable to chloride
218 channels. The presence of cytoplasmic gluconate instead of Cl⁻ caused a decrease in
219 conductance from 296 pS to 82 pS, which indicates that the channels are less permeable
220 to gluconate than to chloride (Fig. 3C, D). The relative permeability ratio of gluconate
221 with respect to chloride (P_{glu}/P_{Cl}) was low and reached 0.1.

222 A characteristic feature of the channels was their activation in the narrow range
223 of voltages, since the open probability of the channels was the highest close to 0 mV
224 (Fig. 3E). The values of this parameter recorded at positive voltages were higher in
225 conditions promoting outward currents carried by Cl⁻ flowing from the extracellular to
226 the cytoplasmic side of the cell membrane than those obtained in the symmetrical Cl⁻
227 concentration. For instance, at 60 mV, the open probability increased from 0.064±0.043
228 to 0.33±0.091 (n=5). The open probability of the channels recorded at positive voltages
229 was also reduced after replacement of extracellular Cl⁻ with gluconate. The value of this
230 parameter recorded at 60 mV was reduced from 0.33±0.091 to 0.068±0.025 (n=5).

231 During the recordings carried out in a NaCl gradient that reduced cation-
232 permeable channel activity at positive voltages (Fig. 1B, 3B) apart from the main open

233 level, three subconductance levels of the anion-permeable channels were observed (Fig.
234 3F). The channel subconductance levels in the presented recordings at positive voltages
235 were 5% (20 pS), 20% (75 pS), and 70% (297 pS).

236 The range of voltages that activate the channels was studied by application of
237 two kinds of ramp voltages: from -80 mV to +80 mV and from +80 mV to -80 mV. The
238 measurements carried out in the symmetrical Cl⁻ concentration proved that the channels
239 were activated in a narrow range of voltages (Fig. 4A, B). Even after application of the
240 Cl⁻ gradient promoting outward currents carried by chloride (Fig. 4C, D), the channels
241 closed at voltages close to 60-70 mV. The ramp protocol used in the measurements of
242 the channel activity after application of the Cl⁻ gradient allowed estimation of the
243 reversal potential, which was close to E_{Cl} (Fig. 4C, D).

244 **Calcium dependence of the channels**

245 Since internal Ca²⁺ activates some channels found in fibroblasts, e.g. non-
246 selective channels from human skin fibroblasts (Galietta *et al.* 1989), or potassium
247 channels from rat cardiac fibroblasts (Choi *et al.* 2008), we decided to study the calcium
248 dependence of all channels recorded in the mouse fibroblasts cell line L929. Calcium
249 dependence was studied in a Ca²⁺-free bath medium by injection of 2 mM Ca²⁺ to the
250 internal site of the membrane during inside-out recordings.

251 The presence of internal calcium was necessary to maintain the activity of
252 nonselective cation channels. These channels were not recorded in the Ca²⁺-free bath
253 medium but injection of Ca²⁺ rapidly (within a few seconds) activated the channels (Fig.
254 5A, upper panel). The channels were also rapidly inactivated after removal of the
255 membrane from the stream of the Ca²⁺-containing solution (Fig. 5A, lower panel). A
256 relatively long time was necessary for activation of small-conductance K⁺ channels

257 (Fig. 5B, upper panel). These channels were also recorded in a Ca^{2+} -free bath medium
258 within tens of seconds after excision or several or more seconds after chelation of Ca^{2+}
259 by EGTA (Fig. 5B lower panel). Such results indicate that the Ca^{2+} binding/unbinding
260 process proceeds more slowly in small-conductance potassium channels than in
261 nonselective cation channels. No calcium dependence was observed in the large-
262 conductance anion channels (Fig. 5C). Injection of Ca^{2+} neither opened the channels at
263 voltages which usually caused their inactivation (Fig. 5C, upper panel) nor changed the
264 channels' activity recorded at voltages close to zero (Fig. 5C, lower panel). The results
265 indicate that voltage but not calcium is the main factor that regulates the activity of
266 large-conductance anion channels.

267 **Discussion**

268 In this study carried out on the membrane of the mouse fibroblast cell line L929,
269 three different ion channel activities were observed. Most often, the activity of
270 nonselective cation channels was recorded. The channel selectivity did not allow
271 distinguishing between sodium and potassium. Similar channels nonselective for cations
272 activated by a platelet-derived growth factor were previously described in mouse
273 fibroblasts in the LMTK⁻ cell line (Frace and Gargus 1989). Apart from the equal
274 selectivity for basic monovalent cations, a common feature of the channels from the
275 LMTK⁻ and L929 cell lines was their conductance amounting to 28 pS for both
276 channels. Another parameter that can be taken into account in the comparison of both
277 channels is their voltage dependence. Channels from the L929 cell line recorded in
278 symmetrical concentration 200 mM NaCl opened with a high open probability at
279 positive voltages (Fig. 1D), while the channels from the LMTK⁻ cell line were voltage
280 independent. On the other hand, the voltage dependence of the channels determined in

281 this study is similar to sodium and potassium nonselective channels from human
282 fibroblasts, which opened with a higher probability at positive voltages and passed the
283 cations with the conductance of 14 to 25 pS (Galietta *et al.* 1989). Moreover, in contrast
284 to the channels from the LMTK⁻ cell line, the channels from the human fibroblasts and
285 L929 cell line were activated by cytoplasmic calcium. It seems that the voltage and
286 calcium dependence of nonselective cation channels is not a common feature of
287 channels from different organisms or even from different cell lines.

288 The second type of the channels recorded in our study was the small-
289 conductance K⁺ channel characterised by low conductance reaching 8 pS (Fig. 2) and
290 Ca²⁺ dependence (Fig. 6B). According to the present knowledge, there are no similar
291 channels in mammalian fibroblasts and it is hard to classify the channels to other known
292 types of channels. The main features of the small-conductance K⁺ channels analysed in
293 this study are similar to small conductance Ca²⁺-activated K⁺ channels (SK channels)
294 encoded by at least three genes: SK1, SK2, and SK3 (Kohler *et al.* 1996). Apart from
295 small unitary conductance (2-20 pS), Ca²⁺ sensitivity (submicromolar concentrations),
296 weak voltage dependence, and susceptibility to blockade by d-tubocurarine and apamin
297 are characteristic for SK channels (Kohler *et al.* 1996, Xia *et al.* 1998, Hirschberg *et al.*
298 1999, Soh and Park 2002). All the three subtypes of SK are present in mouse atrial and
299 ventricular myocytes (Tuleja *et al.* 2005), where heteromeric SK2-SK3 channels
300 contribute to action potential repolarization (Hancock *et al.* 2015). In turn, in mouse
301 urinary bladder, the SK2 gene is expressed and is essential for regulation of the smooth
302 muscle contractility by SK channels (Thorneloe *et al.* 2008).

303 The third type of the channels recorded in our study was the large-conductance
304 anion channel (Fig. 3). Similar channels were recorded and characterized earlier in

305 different cell types, including human fibroblasts (Nobile and Galietta 1988). Apart from
306 the large conductance of the channels from mouse (493 pS in the symmetrical
307 concentration of 200 mM NaCl) and human (300 pS in symmetrical 135 mM NaCl), a
308 common feature of the channels was their similar voltage dependence, since the
309 channels from human fibroblasts were usually open at voltages between -20 to +20 mV
310 and more positive or negative voltages closed the channels. A bell-shaped curve of the
311 open probability with the highest value of this parameter at the voltage close to the
312 reversal potential/zero mV was found in large-conductance anion channels from other
313 types of cultured cells, for instance in human T lymphocytes (Pahapill and Schlichter
314 1992), rabbit colonic smooth muscle (Sun *et al.* 1992), or pigmented ciliary epithelial
315 (PCE) cells (Mitchell *et al.* 1997). Moreover, the activity of a large-conductance
316 channel from PCE was also recorded several minutes after polarization, similar to the
317 one recorded in this study. The next feature of large-conductance channels, similar to
318 the channels recorded in this study, is their low selectivity and nearly equal permeability
319 to gluconate and other anions like I, Br, NO₃, F, SCN, glucuronate, HCO₃, aspartate
320 and acetate (Stumpff *et al.* 2009, Bosma 1989, Dixon *et al.* 1993). The relative
321 permeability ratio of gluconate in respect to Cl⁻ obtained by Stumpff and coworkers
322 from ruminal epithelial cells from sheep ($P_{glu}/P_{Cl} = 0.16$; Stumpff *et al.* 2009), was
323 close to the value of this parameter obtained in our study ($P_{glu}/P_{Cl} = 0.1$). Besides
324 gluconate, low permeability ratios of aspartate and fluoride in respect to chloride were
325 recorded in channels from a mouse B lymphocyte cell line ($P_{aspartate}/P_{Cl} = 0.62$; Bosma
326 1989), and muscle vesicles prepared from *Ascaris suum* ($P_F/P_{Cl} = 0.52$; Dixon *et al.*
327 1993). Large-conductance channels from a mouse B lymphocyte and the channels
328 characterized in this study possess another similar feature - the existence of three

329 subconductance levels. Among the three subconductance levels recorded in mouse B
330 lymphocyte reaching 30 %, 55 %, and 75 % of the total conductance, one was close to
331 that recorded in our study (70 %, Fig. 3F). Subconductance levels were also recorded in
332 the channels from other kinds of cells like the Golgi complex from rat liver (Thompson
333 *et al.* 2002), human L lymphocytes (Pahapill and Schlichter 1992), rat cardiac myocytes
334 (Coulombe and Coraboeuf 1992), rat cortical astrocytes (Jalonen 1993), and rabbit
335 colonic smooth muscle (Sun *et al.* 1992).

336 In conclusion, this study has proved the existence of three different ion channel
337 types in mouse fibroblasts, which exhibit common features with known channels of
338 other cells/cell lines. Three channel types with known physiological functions are the
339 candidates for being active in mouse fibroblasts: non-selective for cations, small-
340 conductance Ca^{2+} -activated K^+ channels (SK), and a large-conductance anion channels.
341 This work is a basis for a more detailed study of the channels from mouse L929 line
342 cells.

343 **Conflicts of Interest**

344 The authors declare that they have no conflict of interest.

345 **Author contributions**

346 All authors have approved the final version of the manuscript and agree to be
347 accountable for all aspects of the work. All persons designated as authors qualify for
348 authorship, and all those who qualify for authorship are listed. Mateusz Koselski
349 developed the conception and design of the work, performed the experiments, analysed
350 and interpreted the data, and wrote the main part of the manuscript. Anna Olszewska
351 participated in writing and reviewing the manuscript. Anna Hordyjewska, Teresa
352 Małecka-Massalska and Kazimierz Trebacz critically reviewed the manuscript. The

353 experiments were performed in the laboratory of the Department of Biophysics,
354 Institute of Biology and Biochemistry, Maria Curie-Skłodowska University, Poland.

355

356 **Acknowledgements**

357 This study was funded by the Scientific Research Fund of Maria Curie-Skłodowska
358 University and the Medical University of Lublin.

359 **References**

- 360 BOSMA MM: Anion channels with multiple conductance levels in a mouse
361 lymphocyte-B cell-line. *J Physiol-London* **410**: 67-90, 1989.
- 362 CHOI S, LEE W, YUN J, SEO J, LIM, I: Expression of Ca^{2+} -activated K^+ channels and
363 their role in proliferation of rat cardiac fibroblasts. *Korean J Physiol Pha* **12**: 51-58,
364 2008.
- 365 COULOMBE A, CORABOEUF E: Large-conductance chloride channels of newborn
366 rat cardiac myocytes are activated by hypotonic media. *Pflug Arch Eur J Phy* **422**: 143-
367 150, 1992.
- 368 DIXON DM, VALKANOV M, MARTIN RJ: A patch-clamp study of the ionic
369 selectivity of the large conductance, Ca-activated chloride channel in muscle vesicles
370 prepared from *Ascaris suum*. *J Mebrane Biol* **131**: 143-149, 1993.
- 371 DOROSHENKO P: High intracellular chloride delays the activation of the volume-
372 sensitive chloride conductance in mouse L-fibroblasts. *J Physiol-London* **514**:437 -446,
373 1999.
- 374 ESTACION M: Characterization of ion channels seen in subconfluent human dermal
375 fibroblasts. *J Physiol-London* **436**: 579-601, 1991.

376 ETCHEBERRIGARAY R, ITO E, OKA K, TOFELGREHL B, GIBSON GE, ALKON
377 DL: Potassium channel dysfunction in fibroblasts identifies patients with Alzheimer
378 disease. *Proc Natl Acad Sci USA* **90**: 8209-8213, 1993.

379 FISKE JL, FOMIN VP, BROWN ML, DUNCAN RL, SIKES RA: Voltage-sensitive
380 ion channels and cancer. *Cancer Metast Rev* **25**: 493-500, 2006.

381 FRACE AM, GARGUS JJ: Activation of single-channel currents in mouse fibroblasts
382 by platelet-derived growth factor. *Proc Natl Acad Sci USA* **86**: 2511-2515, 1989.

383 GALIETTA LJV., MASTROCOLA T, NOBILE M: A class of non-selective cation
384 channels in human fibroblasts. *Febs Lett* **253**: 43-46, 1989.

385 GOODWIN PA, CAMPBELL KE, EVANS BAJ, WANN KT: In vitro patch-clamp
386 studies in skin fibroblasts. *J Pharmacol Toxicol* **39**: 229-233, 1998.

387 HANCOCK JM, WEATHERALL KL, CHOISY SC, JAMES AF, HANCOX JC,
388 MARRION NV: Selective activation of heteromeric SK channels contributes to action
389 potential repolarization in mouse atrial myocytes. *Heart Rhythm* **12**: 1003-1015, 2015.

390 HIRSCHBERG B, MAYLIE J, ADELMAN JP, MARRION NV: Gating properties of
391 single SK channels in hippocampal CA1 pyramidal neurons. *Biophys J* **77**: 1905-1913,
392 1999.

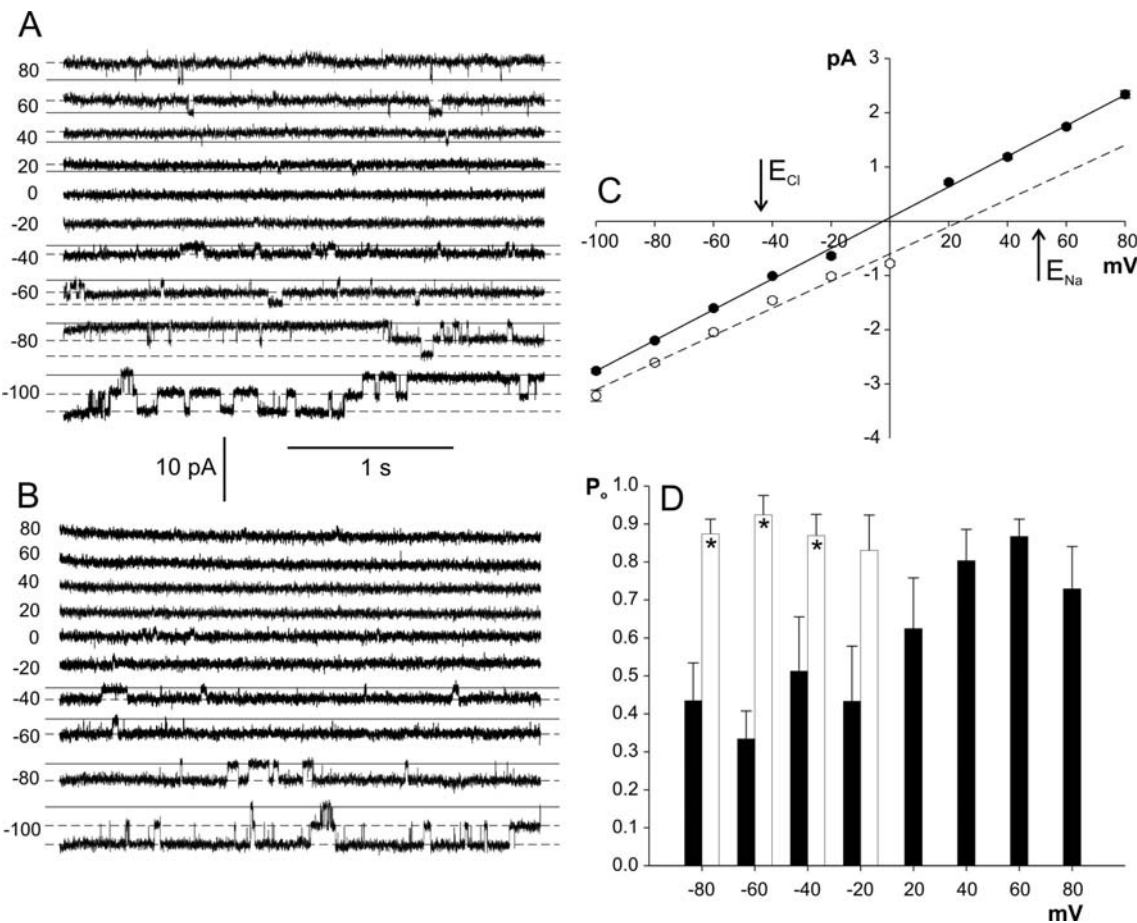
393 HOSOI S, SLAYMAN CL: Membrane voltage, resistance, and channel switching in
394 isolated mouse fibroblasts (L-cells) - a patch-electrode analysis. *J Physiol-London* **367**:
395 267-290, 1985.

396 JALONEN T: Single-channel characteristics of the large-conductance anion channel in
397 rat cortical astrocytes in primary culture. *Glia* **9**: 227-237, 1993.

- 398 KOHLER M, HIRSCHBERG B, BOND CT, KINZIE JM, MARRION NV, MAYLIE J,
399 ADELMAN JP: Small-conductance, calcium-activated potassium channels from
400 mammalian brain. *Science* **273**: 1709-1714, 1996.
- 401 MITCHELL CH, WANG L, JACOB TJC: A large-conductance chloride channel in
402 pigmented ciliary epithelial cells activated by GTP γ S. *J Membrane Biol* **158**: 167-175,
403 1997.
- 404 NOBILE M, GALIETTA LJV: A large conductance Cl⁻ channel revealed by patch-
405 recordings in human fibroblasts. *Biochem Biophys Res Co* **154**: 719-726, 1988.
- 406 PAHAPILL PA, SCHLICHTER LC: Cl⁻ channels in intact human T lymphocytes. *J
407 Membrane Biol* **125**: 171-183, 1992.
- 408 PERES A, STURANI E, ZIPPEL R: Properties of the voltage-dependent calcium-
409 channel of mouse Swiss 3T3 fibroblasts. *J Physiol-London* **401**: 639-655, 1988a.
- 410 PERES A, ZIPPEL R, STURANI E, MOSTACCIUOLO G: A voltage-dependent
411 calcium current in mouse Swiss 3T3 fibroblasts. *Pflug Arch Eur J Phy* **411**: 554-557,
412 1988b.
- 413 PEREZ-REYES E: Molecular physiology of low-voltage-activated T-type calcium
414 channels. *Physiol Rev* **83**: 117-161, 2003.
- 415 REPP H, KOSCHINSKI A, DECKER K, DREYER F: Activation of a Ca²⁺-dependent
416 K⁺ current in mouse fibroblasts by lysophosphatidic acid requires a pertussis toxin-
417 sensitive G protein and Ras. *N-S Arch Pharmacol* **358**: 509-517, 1998.
- 418 SOH H, PARK CS: Localization of divalent cation-binding site in the pore of a small
419 conductance Ca²⁺-activated K⁺ channel and its role in determining current-voltage
420 relationship. *Biophys J* **83**: 2528-2538, 2002.

- 421 STUMPF F, MARTENS H, BILK S, ASCHENBACH JR, GAEBEL G: Cultured
422 ruminal epithelial cells express a large-conductance channel permeable to chloride,
423 bicarbonate, and acetate. *Pflug Arch Eur J Phy* **457**: 1003-1022, 2009.
- 424 SUN XP, SUPPLISSON S, TORRES R, SACHS G, MAYER E: Characterization of
425 large-conductance chloride channels in rabbit colonic smooth-muscle. *J Physiol-London*
426 **448**: 355-382, 1992.
- 427 THEERAKITTAYAKORN K, BUNPRASERT T: Differentiation capacity of mouse
428 L929 fibroblastic cell line compare with human dermal fibroblast. *World Acad Sci Eng*
429 *Technol* **50**: 373-376, 2011.
- 430 THOMPSON RJ, NORDEEN MH, HOWELL KE, CALDWELL JH: A large-
431 conductance anion channel of the Golgi complex. *Biophys J* **83**: 278-289, 2002.
- 432 THORNELOE KS, KNORN AM, DOETSCH PE, LASHINGER ESR, LIU AX, BOND
433 CT, ADELMAN JP, NELSON MT: Small-conductance, Ca^{2+} -activated K^+ channel 2 is
434 the key functional component of SK channels in mouse urinary bladder. *Am J Physiol-
435 Reg I* **294**: R1737-R1743, 2008.
- 436 THOROED SM, BRYAN-SISNEROS A, DOROSHENKO P: Protein phosphotyrosine
437 phosphatase inhibitors suppress regulatory volume decrease and the volume-sensitive
438 Cl^- conductance in mouse fibroblasts. *Pflug Arch Eur J Phy* **438**: 133-140, 1999.
- 439 TUTEJA D, XU DY, TIMOFEEV V, LU L, SHARMA D, ZHANG Z, XU YF, NIE
440 LP, VAZQUEZ AE, YOUNG JN *et al*: Differential expression of small-conductance
441 Ca^{2+} -activated K^+ channels SK1, SK2, and SK3 in mouse atrial and ventricular
442 myocytes. *Am J Physiol-Heart C* **289**: H2714-H2723, 2005.
- 443 XIA XM, FAKLER B, RIVARD A, WAYMAN G, JOHNSON-PAIS T, KEEN JE,
444 ISHII T, HIRSCHBERG B, BOND CT, LUTSENKO S *et al*: Mechanism of calcium

445 gating in small-conductance calcium-activated potassium channels. *Nature* **395**: 503-
446 507, 1998.
447
448
449
450
451
452
453
454
455
456
457
458
459
460
461
462
463
464
465
466
467
468

469 **Figures**

470

471 **Fig. 1.** Activity of nonselective cation channels recorded in the cell membrane from
 472 mouse fibroblasts. (A) Inside-out recordings carried out in 200 Na^+ pipette/ 200 Na^+ bath.
 473 The solid line indicates the closed state of the channels and the dashed line - open states.
 474 The values of holding voltages (in mV) are placed on the left side of the traces. (B)
 475 Recordings obtained after tenfold reduction of the Na^+ concentration in the bath (200
 476 Na^+ pipette/ 20 Na^+ bath). (C) I/V curves obtained in the same conditions as in A (solid line,
 477 $n=10$), and B (dashed line, $n=6$). The arrows indicate the reversal potential for Cl^- and
 478 Na^+ based on the activity of these ions in the solutions as in B. (D) Dependence of the
 479 open probability (P_o) of the channels on the voltage applied. The data were obtained in
 480 the same conditions as in A (black columns, $n=5$) and B (white columns, $n=5$). The

481 asterisks indicate statistically significant differences ($P<0.05$). Statistical significance
482 was evaluated using a *t*-test. The values of P obtained at -80 mV, -60 mV, and -40 mV
483 amounted to 0.003, 0.001, and 0.048, respectively.

484

485

486

487

488

489

490

491

492

493

494

495

496

497

498

499

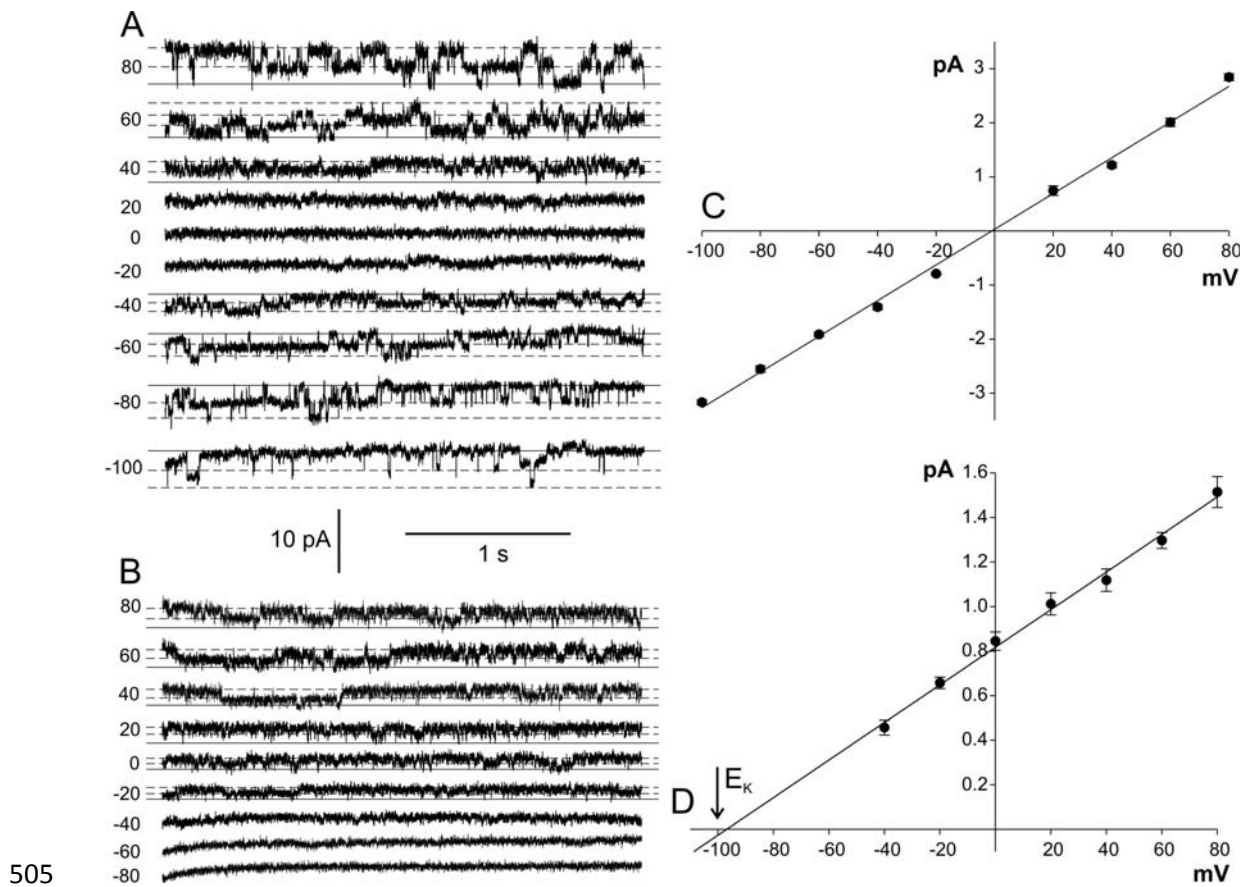
500

501

502

503

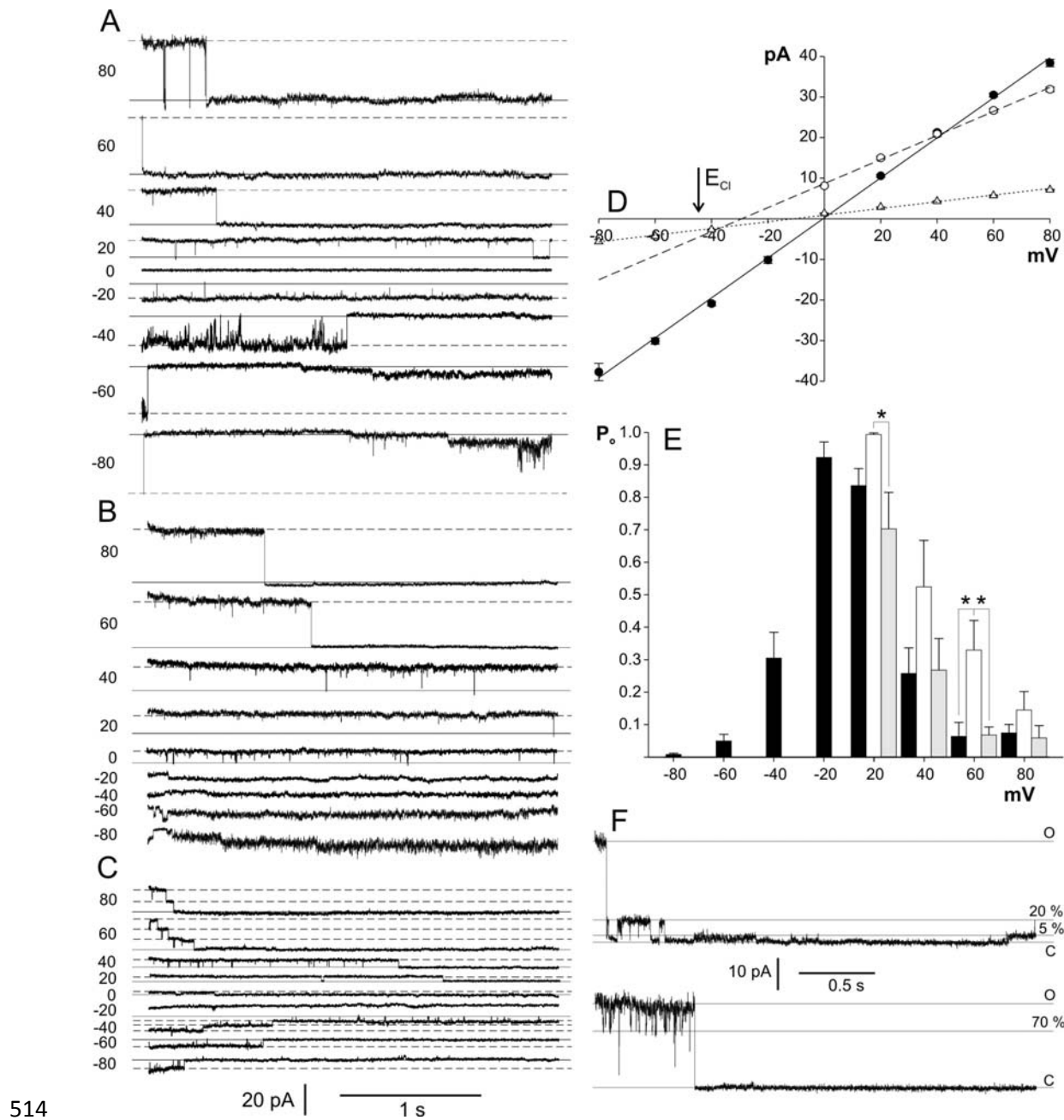
504



505 **Fig. 2.** Permeability of the channels from the cell membrane of mouse fibroblasts to K^+ .

506 (A) Inside-out recordings carried out in 200 Na^+ pipette/ 200 K^+ bath. (B) Inside-out
 507 recordings carried out in the same conditions as in A showing the activity of K^+
 508 selective channels with small conductance. (C, D) I/V curves characterizing the cation-
 509 permeable channels from A (C, $n=5$) and the K^+ selective channels from B (D, $n=5$).
 510

511 The arrow indicates the reversal potential for K^+ calculated from the activity of this ion
 512 in the solutions.
 513

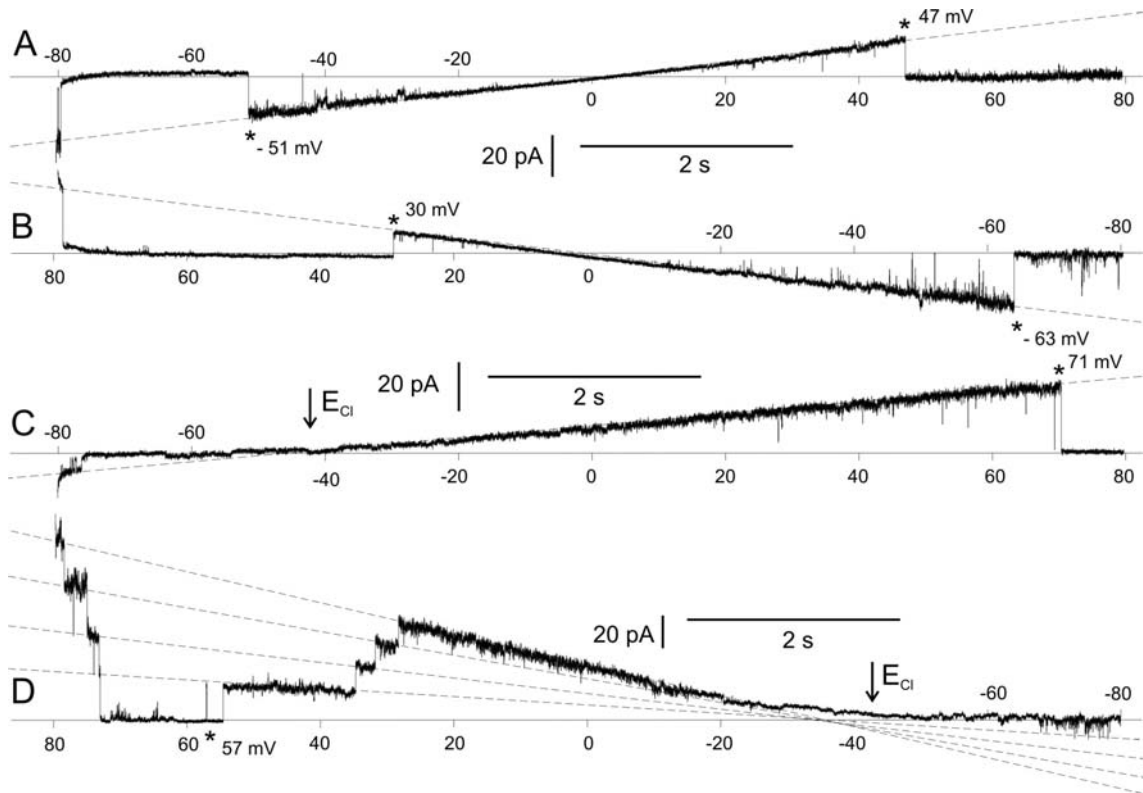


515 **Fig. 3.** Activity of large conductance anion channels recorded in the cell membrane
 516 from mouse fibroblasts. (A) Inside-out recordings carried out in 200 Na^+ pipette/ 200 Na^+
 517 bath. (B) Recordings obtained after tenfold reduction of the Na^+ concentration in the bath
 518 (200 Na^+ pipette/ 20 Na^+ bath). (C) Recordings showing a decrease in single channel
 519 conductance in 200 Glu^- pipette / 32 Cl^- bath. (D) I/V curves obtained in the same
 520 conditions as in A (solid line, $n=6$), B (dashed line, $n=6$), and C (dotted line, $n=6$). The

521 arrow indicates the reversal potential for Cl⁻ calculated from the activity of these ions in
522 the solutions as in B. (E) Dependence of the open probability (P_o) of the channels on the
523 voltage applied. The data were obtained in the same conditions as in A (black columns,
524 $n=5$), B (white columns, $n=5$), and C (grey columns, $n=5$). The asterisks indicate
525 statistically significant differences ($P<0.05$). Statistical significance was evaluated using
526 a one-way ANOVA with Bonferroni pairwise multiple comparison. The values of P
527 obtained at 20 mV amounted to 0.043. The values of P obtained at 60 mV amounted to
528 0.026 (left asterisk) and 0.028 (right asterisk). (F) Subconductance levels of large-
529 conductance anion channels. The inside-out recordings obtained at 80 mV (upper panel)
530 and at 60 mV (lower panel) in 200 Na⁺ pipette/20 Na⁺ bath. C and O indicate closed state
531 and open state, respectively. The subconductance levels (5 %, 20 % and 70 %) are
532 indicated.

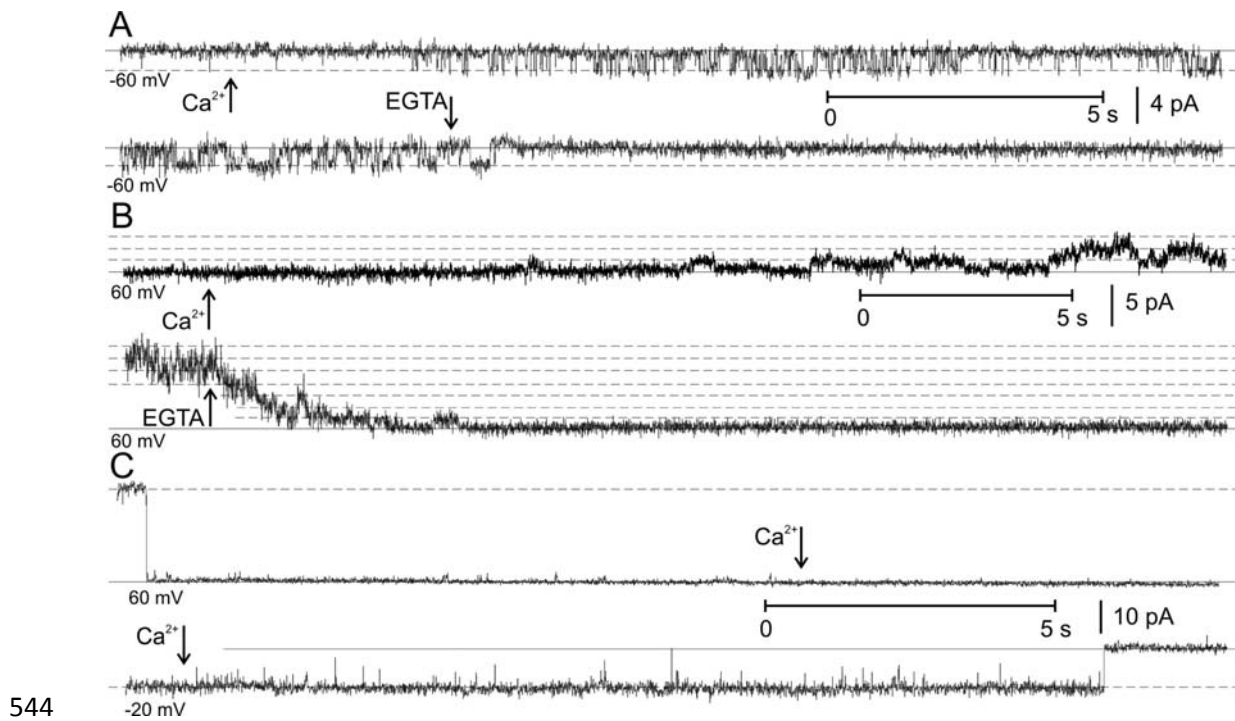
533

534



535

536 **Fig. 4.** Activity of large-conductance anion channels recorded during ramp voltages. (A,
 537 B) Inside-out recordings obtained in 200 Na^+ pipette/ 200 Na^+ bath. (C, D) Recordings
 538 obtained after tenfold reduction of the Na^+ concentration in the bath (200 Na^+ pipette/ 20
 539 Na^+ bath). The arrows indicate the reversal potential for Cl^- calculated from the activity
 540 of this ion in the solutions. The values of the voltage applied (in mV) are placed in the
 541 abscissa axis. The dashed lines indicate the open states of the channels and allow
 542 determining the reversal potential. The asterisks indicate the value of the voltage that
 543 activated the channels.



544 **Fig. 5.** Calcium dependence of different types of ion currents recorded in mouse
 545 fibroblasts. The inside-out measurements were carried out in the absence of Ca^{2+} in the
 546 bath (200 Na^+ , 2 Ca^{2+} _{pipette}/ 200 K^+ , 2 EGTA _{bath}). The calcium dependence was studied
 547 for nonselective cation channels (A), small-conductance K^+ -selective channels (B), and
 548 for large-conductance anion channels (C). The Ca^{2+} -containing solution (200 mM KCl , 4
 549 mM NaCl , 2 mM CaCl_2 , 2 mM MgCl_2 , pH 7.3 buffered with 10 mM HEPES/NaOH)
 550 was placed inside a micropipette connected to the pump. During the inside-out
 551 recordings, the micropipette was brought close to the patch pipette and the solution was
 552 injected. The moment of Ca^{2+} injection is indicated by an arrow. The arrow signed as
 553 EGTA indicates the moment of withdrawal of the patch pipette from the stream of the
 554 injected Ca^{2+} -containing solution. The values of holding voltages are placed at the
 555 bottom of the recordings.

557